INVESTIGATING PERMEABILITY OF POROUS GRAPHENE

by

Alexander MALOZEMOV*

Tomsk State University, Tomsk, Russia

Original scientific paper
https://doi.org/10.2298/TSCI19S2525M

A graphene sheet with regular pores similar to the surface form of boron nitride is simulated be means of crystallographic constructions. The sheet is represented by the aggregate of carbon atoms in the corresponding positions of the crystal structure which do not experience thermal oscillations. Within the framework of the presented approximation, permeability of porous graphene with respect to natural gas components is theoretically analysed. Based on the results obtained, selectivity of separation for methane-helium mixtures is determined.

Key words: *molecular dynamics, porous graphene, potential interaction, differential permeability, gas separation*

Introduction

A graphene-like film of boron nitride is a relatively new promising material in the field of nanotechnology. This material is of extraordinary interest, largely due to its strength and electronic properties. A lot of fundamental research is associated with studies on such properties [1-9]. Production of graphene-like boron nitride became possible due to application of the epitaxy method which consists in using one material as a substrate for production of another material. In this case, boron nitride has the same hexagonal structure as graphene, fig. 1.

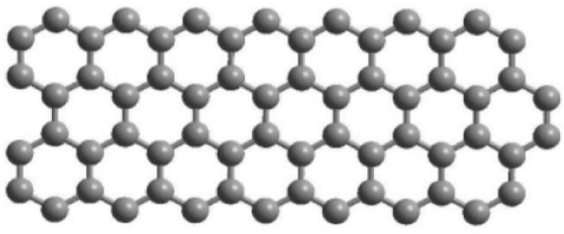

Figure 1. Hexagonal structure of graphene

As a result of steam chemical deposition, it was possible to obtain a two-dimensional material with a thickness of 1-atom which consists of hexagonal cells, as in graphene, but has a porous structure. The pores are cells in the form of a heptagon, fig. 2(a), or an octagon, fig. 2(b).

* Author's e-mail: avmalozemov@gmail.com

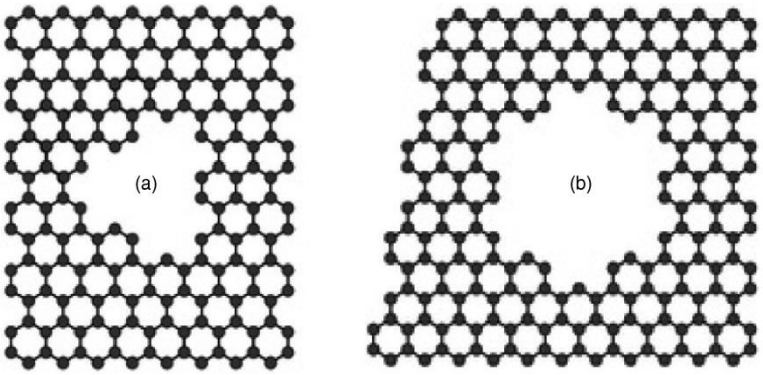

Figure 2. Films of boron nitride with heptagonal (a), and octagonal (b) cells [10]

However, studies have shown that the structure with heptagonal pores is not stable, so the hybrid material with octagonal cells is of a greater interest. The presence of regular pores in the surface form of boron nitride made it possible to use such a structure as a selective filter for separation of natural gas components since a continuous film of boron nitride appears to be impermeable even for lightest components.

Structures obtained from boron nitride are basically similar to carbon structures. However, there are small differences in the scales of the hexa- or pentagonal grids of atoms. Apparently, these differences lead to appearance of regular pores in case of using the epitaxy method, when graphene is used as the substrate. If to use the same method of epitaxy, but to take porous boron nitride as a substrate, it is possible to obtain graphene with regular pores.

The numerical model

In this paper we study permeability of porous graphene with pores similar to those that are found in a film of boron nitride synthesized by the epitaxy method.

Investigations of interaction processes for a moving molecule and atoms of a nanoporous graphene structure are based on application of a mathematical model and numerical methods for solving the fundamental problem of dynamics of a molecule. Interactions between individual atoms or molecules are determined by the classical Lennard-Jones potential. The process of interaction with the structure is described by the law of action independence as the sum of effects from each structure atom on the test molecule under consideration. According to this law, if several forces act on a material point, it acquires acceleration equal to the geometric sum of accelerations which the forces would produce when acting separately. The presented model was tested while studying the process of filtration by carbon nanotubes [11-19].

In the projections on the co-ordinate axis, the equations of motion for the molecule interacting with the carbon structure will be written:

$$m\frac{\mathrm{d}U}{\mathrm{d}t} = X', \quad m\frac{\mathrm{d}V}{\mathrm{d}t} = Y', \quad m\frac{\mathrm{d}W}{\mathrm{d}t} = Z', \quad \text{where} \quad X' = \sum_{j=1}^{N_p} X'_j, \quad Y' = \sum_{j=1}^{N_p} Y'_j, \quad Z' = \sum_{j=1}^{N_p} Z'_j \qquad (1)$$

Here, X', Y', Z' are the projections of the Van der Waals forces resultant from the atoms of the carbon structure which are defined as simple sums of force contributions from the nodes of linear crystals and N_p – the number of atoms in the carbine structure under consid-

eration. Next, we introduce the values X, Y, Z: $mX = X'$, $mY = Y'$, $mZ = Z'$ where m is the mass of the penetrating molecule. Then, in the new variables, eq. (1) can be rewritten:

$$\frac{\mathrm{d}U}{\mathrm{d}t} = X,\ \frac{\mathrm{d}V}{\mathrm{d}t} = Y,\ \frac{\mathrm{d}W}{\mathrm{d}t} = Z,\ \text{where } X = \sum_{j=1}^{N_p} a_j \frac{x - x_j^0}{\rho_j},\ Y = \sum_{j=1}^{N_p} a_j \frac{y - y_j^0}{\rho_j},\ Z = \sum_{j=1}^{N_p} a_j \frac{z - z_j^0}{\rho_j} \quad (2)$$

Here, the zero-index denotes the co-ordinates of the carbon network nodes and a_j – the value of acceleration that the test molecule acquires under the action of the j^{th} atom of the net structure under consideration. This value is expressed through the parameters of the Lennard-Jones potential and the distance to the structure atom:

$$a_j = 24\frac{\varepsilon}{M\rho_j}\left(\frac{\sigma}{\rho_j}\right)^6\left[2\left(\frac{\sigma}{\rho_j}\right)^6 - 1\right] \quad (3)$$

In eq. (3) ρ_j is the distance between the test molecule and the j^{th} atom of the carbon structure, σ and ε are the parameters of interactions between pairs of substances which are included in the *LJ*-potential.

If eq. (2) are supplemented by kinematic relations determining the velocity of the point:

$$\frac{\mathrm{d}x}{\mathrm{d}t} = U,\ \frac{\mathrm{d}y}{\mathrm{d}t} = V,\ \frac{\mathrm{d}z}{\mathrm{d}t} = W \quad (4)$$

we obtain a system of six ODE of the first order with respect to six unknowns: x, y, z, U, V, W. To solve this system, we will use the Runge-Kutta method of the standard fourth-order accuracy.

In the case when the system under investigation consists of dissimilar molecules (atoms), the parameters ε and σ satisfy the Lorentz-Berthelot mixing rule.

The single-layer nanoporous structure

A model of a single-layer heptagonal porous graphene structure consisting of hexagonal cells with octagonal pores is shown in fig. 3.

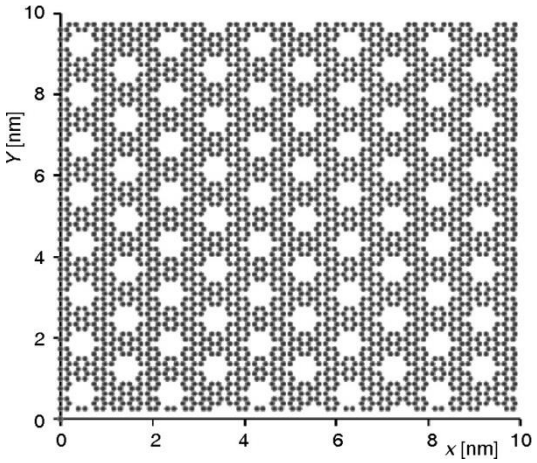

Figure 3. Model of porous graphene structure

Since the distance between carbon atoms in such a structure, as in graphene, is 0.142 nm, while the size and configuration of the pores remain unchanged, permeability of porous graphene is studied by the statistical method. The structure under consideration is divided into equal cells, each including a pore, fig. 4.

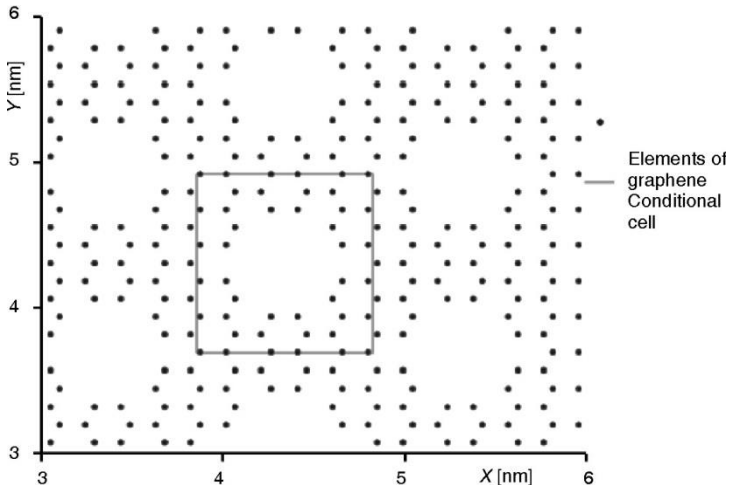

Figure 4. Investigated cell of porous graphene structure

The cell under investigation is divided into several parts. Permeability of the structure is tested by a molecule – an atom of the gas phase which has co-ordinates coinciding with the cell node at the initial instant. Permeability of the system as a whole is estimated as the number of nodes at which the particle passes through the intermolecular barrier in relation to the total number of nodes of the grid under consideration. Thus, in the case of CH_4 molecules, the structure turned out to be absolutely impermeable, while in the case of helium atoms, permeability was equal to 2.7%, fig. 5. Consequently, separation selectivity for CH_4-helium mixtures is $\chi = D_{He} / D_{CH_4} = \infty$.

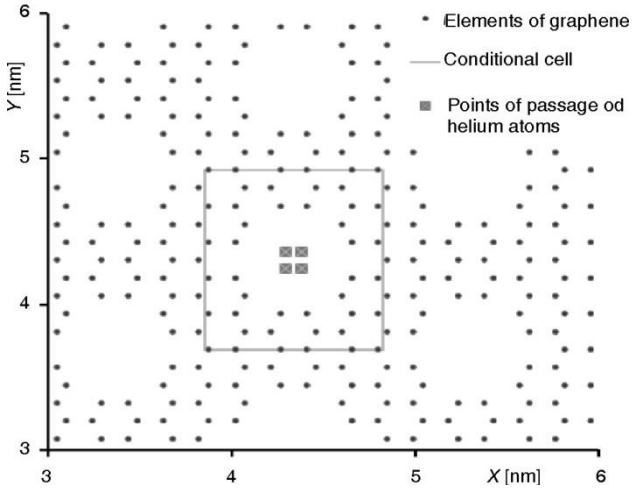

Figure 5. Permeability of porous graphene structure with respect to helium atoms at rms velocity

The existence of a permeability window for the passing component is clearly shown in fig. 6. The helium atoms shifted at the initial time point by some distance (x_0 = 4.30, x_0 = 4.38 nm) from the centre of the pore (x_0 = 4.34 nm) pass through the energy barrier, despite the fact that the particle is located within the pore area, further displacement (x_0 = 4.24, x_0 = 4.44 nm) does not allow passage of helium atoms, which is ensured by the contribution of the $(\sigma/\rho)^{12}$-term in the Lennard-Jones potential characterizing repulsion.

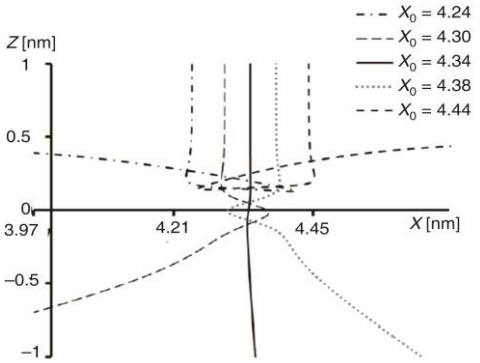

Figure 6. Projection of helium atoms' trajectories when displaced from centre of pore at initial time instant at mean square velocity

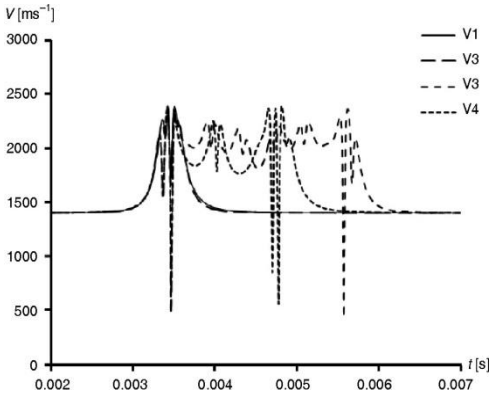

Figure 7. Velocity of helium atom when interacting with elements of porous graphene

Conclusion

Permeability of a porous graphene net with respect to CH_4 molecules and helium atoms was studied. A mathematical model of the interaction between test particles and elements of nanoporous graphene was presented. The obtained results allow drawing a conclusion that the material under study has high selectivity with respect to CH_4-helium mixtures since it is absolutely impermeable to CH_4 molecules. At the same time, a filter having porous graphene as its element appears to be low-productive since its relative permeability for helium was 2.7%.

References

[1] Ismail, A. F., *et al.*, Gas Separation Membranes: Polymeric and Inorganic, Springer, New York, USA, 2015
[2] Geim, A., *et al*., The Rise of Grapheme, *Nature Materials, 6* (2007), Mar., pp. 183-191
[3] Schwierz, F., Graphene Transistors, *Nature Nanotechnology, 5* (2010), May, pp. 487-496
[4] Gong, G., *et al.*, Field Effect in Epitaxial Graphene on a Silicon Carbide, *Applied Physics Letters, 90* (2007), 25, 253507
[5] Pang, J., *et al*., Field Effect in Epitaxial Graphene on a Silicon Carbide, *Thermal Science, 17* (2013), 5, pp. 1449-1452
[6] Geim, A., Graphene: Status and Prospects, *Science, 324* (2009), 5934, pp. 1530-1534
[7] Williams, J. R., *et al*., Quantum Hall Effect in a Gate-Controlled p-n Junction of Grapheme, *Science, 317* (2007), 5835, pp. 638-641
[8] Terao, T., *et al*., Alignment of Boron Nitride Nanotubes in Polymeric Composite Films for Thermal Conductivity Improvement, *Journal of Physical Chemistry C, 114* (2010), 10, pp. 4340-4344
[9] Taric, M. R., et al., Monitoring and Neural Network Modeling of Cutting Temperature During Turning Hard Steel, *Thermal science, 22* (2018), 6A, pp. 2605-2614
[10] ***, Graphene and Hexagonal Boron Nitride: Joint Prospects in Nanoelectronics, https://www.en.wikipedia.org/wiki/Graphene_boron_nitride_nanohybrid_materials

[11] Bubenchikov, M. A., *et al*., Potentsial Vzaimodeystviya Otkrytoy Nanotrubki i Yego Pronitsayemost': Modelirovaniye Molekulyarnoy Dinamiki, (The Interaction Potential of an Open Nanotube and its Permeability: Molecular Dynamics Simulation – in Russian), *Proceedings*, EPJ Web of Conferences, 2016, Vol. 110, 01016
[12] Qina, D.-H., *et al*., Magnetic Domain Structure in Small Diameter Magnetic Nanowire Arrays, *Applied Surface Science, 239* (2005), 3-4, pp. 279-284
[13] Gusev, A. I., *Nanomateriali, Nanostrukturi, Nanotekhnologii*, (Nanomaterials, Nanostructures, Nanotechnologies – in Russian), 2nd ed., Fizmatlit, Moscow, 2009
[14] ***, Ordered Carbon Nanostructures and Areas of their Practical Application, http://www.tehnar.net.ua/uporyadochennyie-uglerodnyie-nanostrukturyi-i-oblasti-ih-prakticheskogo-primeneniya/
[15] Solaymani, A., *et al*., Effect of Pressure on Gas Permeability and Selectivity of Carbon Nano-Structure/Polyacrylonitrile Mixed Matrix Membrane, *Science of Advanced Materials, 5* (2013), 6, pp. 656-662
[16] ***, Carbine, https://www.dic.academic.ru/dic.nsf/ruwiki/61210
[17] Klykov, I. I., *et al*., Molekulyarnoye Dvizheniye Cherez Otkrytuyu Karbonovuyu Trubku, (Molecular Movement through an Open Carboxylic Tube, News of Higher Educational Institutions – in Russian), *Physics, 57* (2014), 8/2, pp. 161-164
[18] Malozemov, A. V., *et al*., Matematicheskoye modelirovaniye Differentsial'noy Pronitsayemosti Uglerodnykh Nanotrubok, (Mathematical Modelling of Differential Permeability of Carbon Nanotubes – in Russian), *Proceedings*, International Conference on Mechanical Engineering, Automation and Control Systems, Tomsk, Russia, 2014
[19] Bubenchikov, M. A., *et al*., Issledovaniye Pronitsayemosti Uglerodnykh Nanotrubok, (Research on Permeability of Carbon Nanotubes – in Russian), *Proceedings*, MATEC Web of Conferences, 2017, Vol. 110, 01016

Paper submitted: September 5, 2018
Paper revised: November 25, 2018
Paper accepted: December 1, 2018